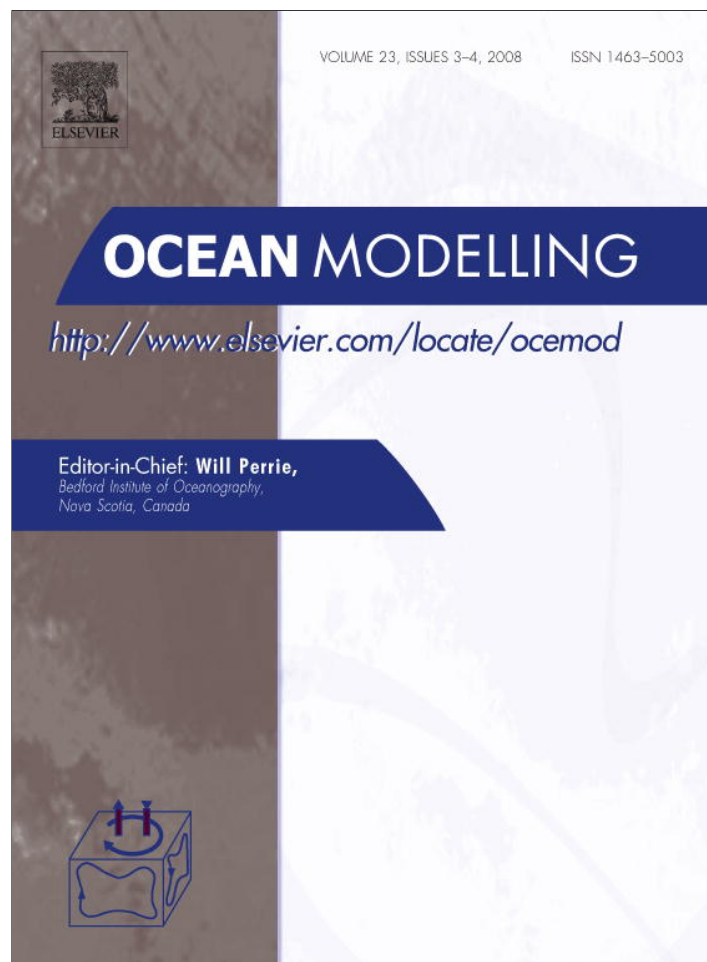


Provided for non-commercial research and education use.
Not for reproduction, distribution or commercial use.



This article appeared in a journal published by Elsevier. The attached copy is furnished to the author for internal non-commercial research and education use, including for instruction at the authors institution and sharing with colleagues.

Other uses, including reproduction and distribution, or selling or licensing copies, or posting to personal, institutional or third party websites are prohibited.

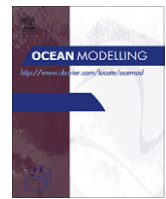
In most cases authors are permitted to post their version of the article (e.g. in Word or Tex form) to their personal website or institutional repository. Authors requiring further information regarding Elsevier's archiving and manuscript policies are encouraged to visit:

<http://www.elsevier.com/copyright>



Contents lists available at ScienceDirect

Ocean Modelling

journal homepage: www.elsevier.com/locate/ocemod

Zonal versus meridional velocity variance in satellite observations and realistic and idealized ocean circulation models

Robert B. Scott^{a,*}, Brian K. Arbic^a, Christina L. Holland^a, Ayon Sen^{a,b}, Bo Qiu^c

^a*Institute for Geophysics, Jackson School of Geosciences University of Texas at Austin, J.J. Pickle Research Campus, Building 196 (ROC), 10100 Burnet Road (R2200), Austin, TX 78759, USA*

^b*Westwood High School, 12400 Mellow Meadow Drive, Austin, TX 78750, USA*

^c*Department of Oceanography, University of Hawaii at Manoa, 1000 Pope Road, Honolulu, HI 96822, USA*

ARTICLE INFO

Article history:

Received 19 January 2008

Received in revised form 2 April 2008

Accepted 21 April 2008

Available online 17 May 2008

Keywords:

Quasigeostrophic turbulence

Anisotropy

Jets

Turbulent diffusion

ABSTRACT

Global, high-quality, satellite-based observation of oceanic currents over the past 13 years has revealed ubiquitous quasi-horizontal eddies in the mesoscale (tens to hundreds of kilometers), confirming the view of a highly turbulent ocean suggested by observational programs in the 1970s. Idealized quasigeostrophic turbulence models suggest mesoscale turbulent flow can vary between isotropic, and highly anisotropic zonal jets. Here we compare the zonal and meridional velocity variance from satellite altimetry. We find that, for an unexplained reason and despite the chaotic nature of turbulence, the surface flow is organized into mesoscale patches where either zonal or meridional velocity variance dominates. The patches persist over 13 years, much longer than the turbulent timescale of a few months. Implications include potentially highly anisotropic redistribution of tracers by the mesoscale flow. Zonally averaged velocity variances reveal a slight preference for meridional over zonal velocity variance. Realistic primitive equation models succeed in reproducing both the patchy structure in local preference for either zonal or meridional velocity variance, and the zonally averaged preference for meridional variance. Idealized models of fully developed, quasigeostrophic turbulence fail in both regards.

© 2008 Elsevier Ltd. All rights reserved.

1. Introduction

Observational programs in the 1970s, for example MODE (e.g. McWilliams, 1976) and POLYMODE (e.g. McDowell, 1986 and references in the same issue), revealed a turbulent ocean filled with quasi-horizontal eddies in the mesoscale (tens to hundreds of kilometers). Oceanic eddies stir nutrients, pollutants and other tracers about 100 times more effectively in the horizontal than in the vertical. The horizontal anisotropy properties of eddies determine their relative mixing effectiveness in the zonal and meridional directions. Since the most energetic oceanic flow is at the surface, and since the surface is much better observed than the deeper flow, we will focus on characterizing anisotropy of the surface mesoscale flow.

Turbulent mesoscale flow of the ocean, like that of the atmosphere of Earth and other planets, is strongly affected by density stratification and rotation of the planet. A rich theory has developed over the last 40 years to explain stratified and rotating turbulence (Danilov and Gurarie, 2000; Vallis, 2006). Buried within the complexity of chaotic, random instantaneous fluid motions, the average properties reveal organizing principles of the flow. Nonlin-

ear interactions between different length scales drive a cascade that redistributes energy between different length scales (Frisch, 1995). The (horizontal) quasi-two-dimensionality of the flow induced by rotation and stratification is responsible for directing the flow of energy toward larger spatial scales in the counterintuitive inverse energy cascade (Batchelor, 1953; Fjortoft, 1953). Anisotropy in the inverse cascade arises from a gradient in the mean potential vorticity (PV), the most studied example being the β -effect, which arises from the meridional gradient in the Coriolis parameter ($\beta = \partial f / \partial y$) due to the curvature of the Earth. The β -effect weakens the cascade into large meridional (but not zonal) length scales. This leads to a preference for zonally elongated eddies, and zonally oriented jets, in both freely decaying horizontally homogeneous turbulence (Rhines et al., 1977; Vallis and Maltrud, 1993; Galperin et al., 2006) and homogeneous turbulence forced by a vertically sheared eastward mean flow (Panetta, 1993). These model experiments help to explain the familiar westerly jet stream of Earth's atmosphere and the clouds of Jupiter stretched into zonal bands. In the ocean there are PV gradients associated with vertical shear of the mean flow, which in general have a meridional component. Arbic and Flierl (2004a) found that when the shear-induced PV gradients in turbulence forced by a nonzonal mean flow are smaller than β then eddies are zonally elongated, but are more isotropic when shear-induced PV gradients are comparable to β . It is

* Corresponding author. Tel.: +1 512 471 0375; fax: +1 512 471 8844.
E-mail address: rscott@ig.utexas.edu (R.B. Scott).

noteworthy that despite the wide range of parameters considered by Arbic and Flierl (2004a), they never found a regime where the meridional velocity variance dominated over the zonal velocity variance. Many other complications that exist in the real ocean are often not taken into account in the theory or in the idealized numerical experiments cited above. Complex topography and coastlines, spatial inhomogeneity of stratification, and complex patterns of surface wind forcing are among these complicating factors.

Observational study of the anisotropy of oceanic eddies requires two-dimensional fields of ocean currents observed over a time period much longer than the approximately 2-week decorrelation time (LeTraon et al., 2001) of oceanic eddies. Traditional measurements from moored instruments provide time series at select points only. Schmitz (1988) found, for example, the relative energy in the meridional and zonal near surface flow can vary greatly across the Kuroshio Extension at 165°E, but this anisotropy changed from one year to another. A mooring in the Gulf Stream also revealed a similar vacillation between near surface zonal and meridional energy (Schmitz et al., 1988). Hogg (1988) finds a similar variation in abyssal current anisotropy across the Gulf Stream at 55°W. Zang and Wunsch (2001) found that 80% (92%) of 105 moorings had the zonal and meridional current variances within a factor of two (three) of each other. However, even for the latter study, the number of these moorings is far too limited to construct global maps of current anisotropy, and the deployments typically too short to confirm their persistence. Only with satellite altimetry is global analysis of anisotropy and its persistence possible. Satellite based altimeters measure the sea-surface height, from which one can infer the geostrophic currents.

Galperin et al. (2004) discovered alternating, zonally elongated bands in the 5-year average zonal velocity field at 1000 m depth of a high-resolution simulation of the OfES model. More recently, Maximenko et al. (2005) applied a 126-day average to the zonal geostrophic velocity from satellite altimetry, revealing zonal, jet-like structures buried in the predominant eddy field. See Galperin et al. (2006) for further theoretical developments explaining the jets in the context of “zonation”, resulting from anisotropic inverse cascades.

Here we focus on velocity anomalies, since most of the kinetic energy in the ocean is in the time variable flow (hereafter “eddy field” or simply “eddies”) on timescales similar to or longer than about 100 days (Zang and Wunsch, 2001, Fig. 7). In the next section we describe diagnostics we use to characterize the relative strength of zonal and meridional velocity variances, M , and the anisotropy properties, M_n . In Section 3 we compare the properties of M found using satellite altimeter data, a state-of-the-art realistic primitive equation model, and an idealized quasigeostrophic (QG) model. The main finding is the discovery of persistent mesoscale structures in M . In Section 4 we speculate on the origin of these persistent structures. We conclude in Section 5 with a discussion of some implications for ocean modelling and parameterizing turbulent diffusion.

2. Methods

We want to characterize the anisotropy of the World Ocean, and any preference for zonal currents over meridional currents in particular. We use a diagnostic technique that characterizes the preference for zonal or meridional current anomalies over all space and time scales revealed by satellite altimetry. We calculated the quantity

$$M = \frac{\langle u^2 - v^2 \rangle}{\langle u^2 + v^2 \rangle}, \quad (1)$$

where u and v are the zonal and meridional current velocity anomalies, and $\langle \cdot \rangle$ denotes time averaging. In an isotropic flow, each direction would have identical variance, so $M = 0$. Thus departures of M from zero result from anisotropy in the mean statistics of the current anomalies. The normalization by twice the eddy kinetic energy ensures that $-1 \leq M \leq 1$. A similar diagnostic was recently used to investigate oceanic anisotropy on large scales by replacing our temporal average with a spatial average over large subregions of the North Pacific (Huang et al., 2007). They investigated the influence of timescale upon their measure of basin-scale anisotropy, and found close to isotropy with no temporal averaging, and that the longer the temporal average used the more anisotropic the flow was. In idealized geostrophic turbulence models (Arbic and Flierl, 2004a), M when averaged over the model domain is always positive and can be as large as 0.5–0.7 depending on the strength of planetary β .

While the diagnostic M has the advantage of being simple, and well suited to compare the strength of the zonal versus meridional velocity variance, it has the disadvantage that flow persistently oriented at 45° to a meridian would yield $M = 0$, despite the extreme anisotropy. To address the anisotropy more generally, we also looked at the velocity variance ellipses. Variance ellipses are found from diagonalizing the velocity covariance matrix $\langle u_i u_j \rangle$, where $i, j \in \{1, 2\}$ indicate the zonal and meridional directions. From the diagonal covariance matrix, we can define our anisotropy measure,

$$M_n = \frac{\langle u^2 - v^2 \rangle}{\langle u^2 + v^2 \rangle}, \quad (2)$$

where $\langle u^2 \rangle$ is chosen to be the larger of the two diagonal terms, so that $0 \leq M_n \leq 1$. Now $M_n = 0$ for purely isotropic flow, and $M_n = 1$ for purely directional flow.

3. Results

3.1. Satellite altimeter observations

We use 13 years of the reference altimeter product produced by Ssalto/Duacs and distributed by Aviso, with support from CNES, which merges measurements from two simultaneously operating satellites onto a 1/3° Mercator grid (LeTraon et al., 1998, 2001; Ducet et al., 2000). Water depths less than 1000 m were omitted in our analysis, both because the altimeter data is more accurate in the deep water, and also because in general the deeper water is farther from the coast where M might reflect the steering of currents by the coastline. Altimeters provide sea surface height measurements along the ground tracks at much higher resolution than the spacing between ground tracks, which can be over 300 km for TOPEX/Poseidon (Chelton et al., 2001, Fig. 61). For most latitudes the altimeter ground tracks are closer to north–south than east–west (Chelton et al., 2001, Fig. 59), providing higher resolution of meridional derivatives than zonal derivatives. Thus the zonal geostrophic velocities are inherently better resolved at most latitudes. However, combining multiple satellite measurements and gridding with equal meridional and zonal decorrelation scales poleward of 14° reduces the inherent sampling discrepancy between zonal over meridional velocity (Ducet and LeTraon, 2001). Favorable comparison with moorings and drifters indicates that the merged two-satellite data can be used for anisotropy studies (Ducet et al., 2000).

The most surprising result emerged outside the Tropics from examination of anisotropy at individual grid points. Fig. 1 displays the global map of M averaged over the 13-year time period, October 11, 1992 through January 21, 2006. The extratropical M field reveals anisotropic eddy velocity fields, with small-scale structure. The upper ocean is well-known to contain chaotic, turbulent flows

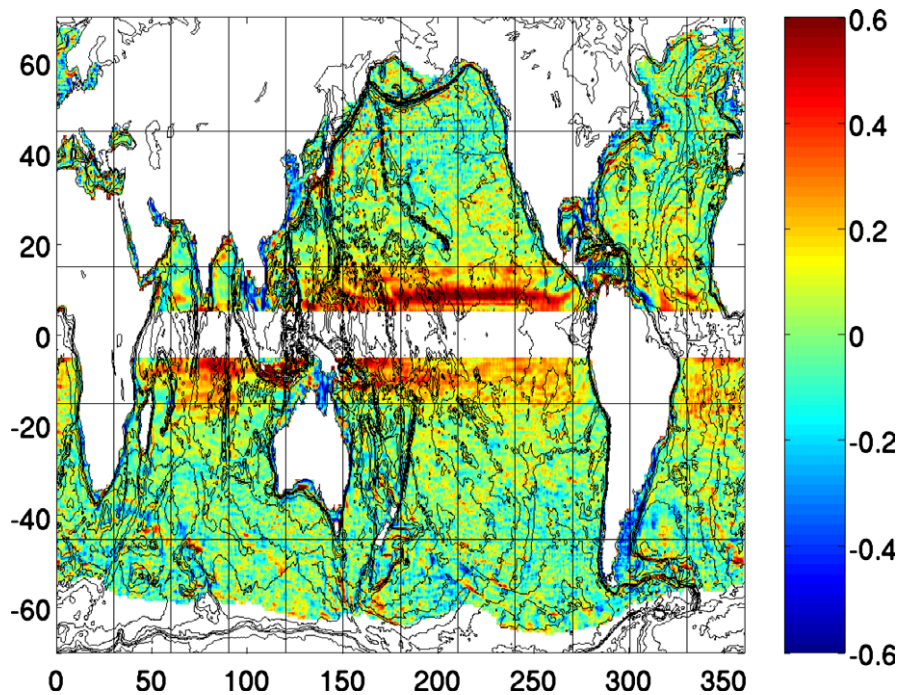


Fig. 1. Thirteen-year average M (October 11, 1992 through January 21, 2006) from satellite altimetry. For depths greater than 1000 m, the two 6-year average M fields (January 2, 1994 through December 31, 1999 and January 2, 2000 through December 31, 2005) are spatially correlated at $r = 0.55$ globally and $r = 0.41$ for latitudes poleward of 25° . Higher correlations found when including shallower depths. Contours are bottom topography with $CI = 1000$ m.

with coherent vortices of spatial scale 50–100 km and timescales typically much less than 100 days: altimeter derived surface velocity decorrelation timescales are typically less than about 20 days (Stammer, 1997, Fig. 17), while the decay time of propagating features is almost everywhere less than 60 days (Jacobs et al., 2001, Plate 6). Well away from coastlines and strong mean currents that might conceivably organize the turbulent flow, we might have thought the turbulence would smear out any flow structures smaller than the scale of the gyre circulations. Yet the M field in Fig. 1 reveals the organization of a turbulent flow over timescales much longer than the inherent timescale of the turbulent fluctuations. In the tropics, M is mostly positive, consistent with the well-known predominantly zonal currents and Rossby waves.

Because eddy kinetic energy is typically much larger than the mean kinetic energy, one might ask whether the features in Fig. 1 are artifacts of single, strong, transient eddies leaving a noticeable signal in the 13-year mean. If we averaged long enough, would the structures in M in Fig. 1 be smeared away? Given the limitations of data duration, we checked the statistical significance by calculating M for the two 6-year time periods January 2, 1994 through December 31, 1999 and January 2, 2000 through December 31, 2005. If the structures in M for a given 6-year average were the result of single, strong, transient eddies, then the structures would be different in detail for the other 6-year period, having resulted from *different* transient eddies. (While eddies can live for up to a few years (Puillat et al., 2002), they are not stationary but propagate away within a few months (Jacobs et al., 2001).) The spatial correlation between these two M fields from two different 6-year periods was $r = 0.55$ for depths greater than 1000 m and higher when shallower depths were included. Given the small-scale structure we estimate that there are thousands of degrees of freedom over the World Ocean. Therefore $r = 0.55$ is statistically significant at much better than the 0.001 level. The spatial correlation is higher in the Tropics, but extratropical correlation is still very highly significant, with $r = 0.41$. The visual correspondence

between the M fields from the two independent 6-year periods was striking. For example, Fig. 2 shows M in the Southern Ocean, east of New Zealand.

Gridded altimeter data from one satellite tends to underestimate the meridional velocities, at length scales smaller than the track spacing, because the ground tracks are oriented more in the meridional direction everywhere except at high latitudes (Ducet and LeTraon, 2001). Furthermore, the meridional velocity has more uncertainty (Schlax and Chelton, 2003). These issues raise the question whether two satellites are enough to capture accurately the M field. Fortunately, for the latter 6-year period, the Aviso “updated” product merges 3–4 satellites and has much improved mapping capability (Pascual et al., 2007). A root-mean-square, rms, discrepancy of 0.06 was found between M from the updated product (not shown) and from the 2-satellite “reference” product, compared to an rms value of M itself of 0.21. Furthermore, their zonal averages were visually indistinguishable between 60°S and 60°N . Higher latitudes were noisy, perhaps contaminated by sea-ice effects.

While the upper ocean may be dominated by mesoscale turbulent flows with timescales typically less than 100 days (Stammer, 1997; LeTraon et al., 2001; Jacobs et al., 2001), larger and longer scales do exist. To confirm that the mesoscale part of the flow is responsible for the persistent M fields, we removed timescales longer than 105 days and spatial scales larger than 2° longitude from the altimeter currents. In particular, we removed a 15-week running mean from the updated, AVISO currents. We also removed the large scales by subtracting the velocity field smoothed with a Gaussian filter of width 2° longitude (6 grid points), and similar meridional width, convolved over a 19×19 grid point region on the $1/3^\circ$ longitude Mercator grid. The two 6-year periods between 1994–1999 and 2000–2005 had M fields at depths greater than 1000 m that were correlated at $r = 0.66$ globally, and $r = 0.50$ poleward of 25° latitude. The mesoscale anisotropy seems to be slightly *more* persistent than anisotropy in the full anomalies relative to the 6-year mean.

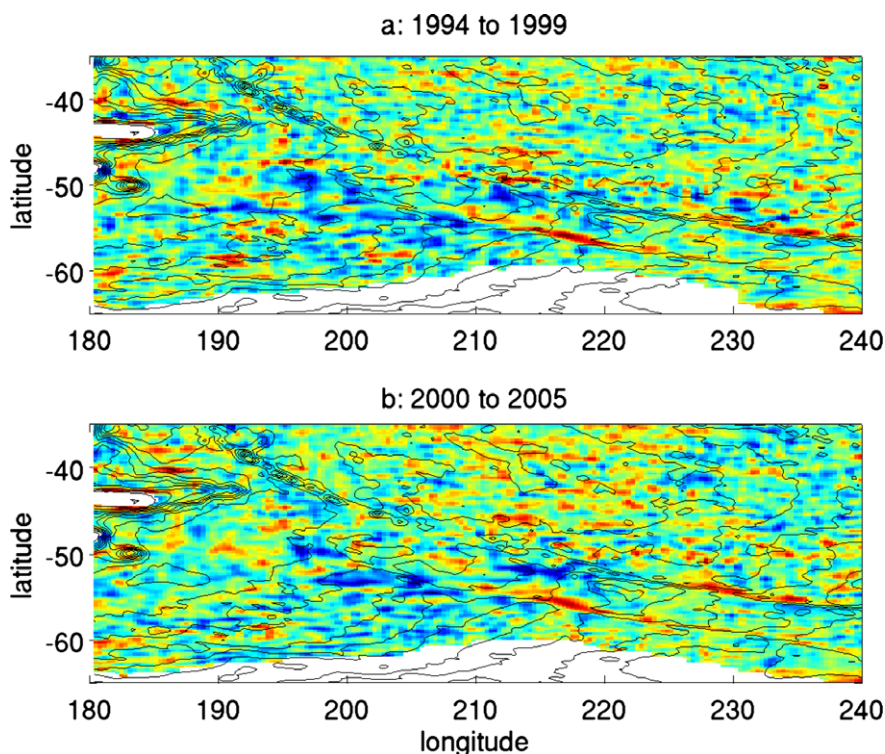


Fig. 2. Six-year mean M from satellite altimetry for the South Pacific: (a) for period January 2, 1994 through December 31, 1999; (b) for period January 2, 2000 through December 31, 2005. Contours are bottom topography with $CI = 500$ m. This region, with spatial correlation between fields in (a) and (b) of $r = 0.34$, is slightly less persistent than typical extratropical regions, but still highly statistically significant.

Besides assessing the spatial correlation between M fields averaged over separate 6-year periods, we also address the statistical significance of the small-scale anisotropy in surface velocity variance in the more standard way by estimating the standard error of $\langle u^2 - v^2 \rangle$. Assuming Gaussian statistics and a decorrelation time of 14 days (LeTraon et al., 2001), we calculated $\langle u^2 - v^2 \rangle$ normalized by its standard error using the updated AVISO velocity fields with 15-week running mean removed. The results are plotted in Fig. 3. Almost one-third of the extratropical World Ocean was found to have $\langle u^2 - v^2 \rangle$ greater than twice its standard error (significant at the 2-sigma level, or with 95% confidence assuming Gaussian statistics). The fields do not appear to be dominated by statistical noise. To assess whether the results are dominated by measurement noise, we assess M in a high-resolution state-of-the-art primitive equation ocean model in Section 3.2.

Recall that there are some advantages to considering M_n , defined in Eq. (2). In Fig. 4 we have contoured M_n for the 6-year period from January 2000 through December 2005. For this M_n field, the temporally and spatially high-pass filtered velocity fields were used, in order to isolate the effects of mesoscale flow. The M_n field is not as persistent as M , since the spatial correlation with the earlier 6-year period was only $r = 0.33$ (for water depths greater than 1000 m and both the extratropics and the World Ocean). Note there does seem to be some grid noise evident just north of the Equator in the eastern-central Pacific. We are not sure the origin of this, but because it appears isolated, it is unlikely to affect the global result.

From the variance ellipses, we found the orientation of the major axis was also persistent and patchy. In Fig. 5 we plot the angle of the major axis, measured anticlockwise from zonal. The spatial correlation with the earlier 6-year period is $r = 0.17$ for depths greater than 1000 m. While lower than other spatial correlations, this is still highly statistically significant. The red shades in the midlatitudes indicate flow preferentially oriented near the merid-

ional direction. This anticipates the preference for $M < 0$ that we find in the zonally averaged results below. (Note that the orientation angle is modular 180° , so angles $\sim -90^\circ$ and $\sim +90^\circ$ are similar. The modularity of the orientation angle may partially explain its lower spatial correlation between time periods. Taking the spatial correlation of the absolute value of the angles between the two 6-year periods was more than double, $r = 0.40$.)

3.2. Realistic primitive equation model results

It is important to verify the M from altimeter data with independent data that has different error characteristics. To this end we calculated M from a state-of-the-art near global (75°S to 75°N) Ocean General Circulation Model for the Earth Simulator, OfES (Sakuma et al., 2003). The OfES model is based on MOM3, has 54 vertical levels and a horizontal grid spacing of $1/10^\circ$. We analyzed the last 10 years of the 50 year simulation, which started from annual mean observed temperature and salinity fields and with zero velocity. It was forced with monthly mean NCEP/NCAR reanalysis (Kistler et al., 2001) momentum, heat and salinity fluxes. The surface salinity field was relaxed to monthly mean climatology. As such, insofar as the M field is related to the surface forcing, the M field may be artificially persistent due to the lack of interannual variability in the forcing. We used one snapshot of the sea-surface height field each month to infer the geostrophic surface velocities, from which we calculated M . Because these snapshots will contain variations not due to geostrophic motions, it was important to compare these results with those obtained by first averaging snapshots of sea-surface height from the first 5 days of each month, and then calculating geostrophic velocities; virtually identical results (not shown) were obtained.

The OfES based M are plotted in Figs. 6 and 7, corresponding to years 41–45 and years 46–50, respectively. The main result is confirmed – small-scale patchy structures are found throughout the

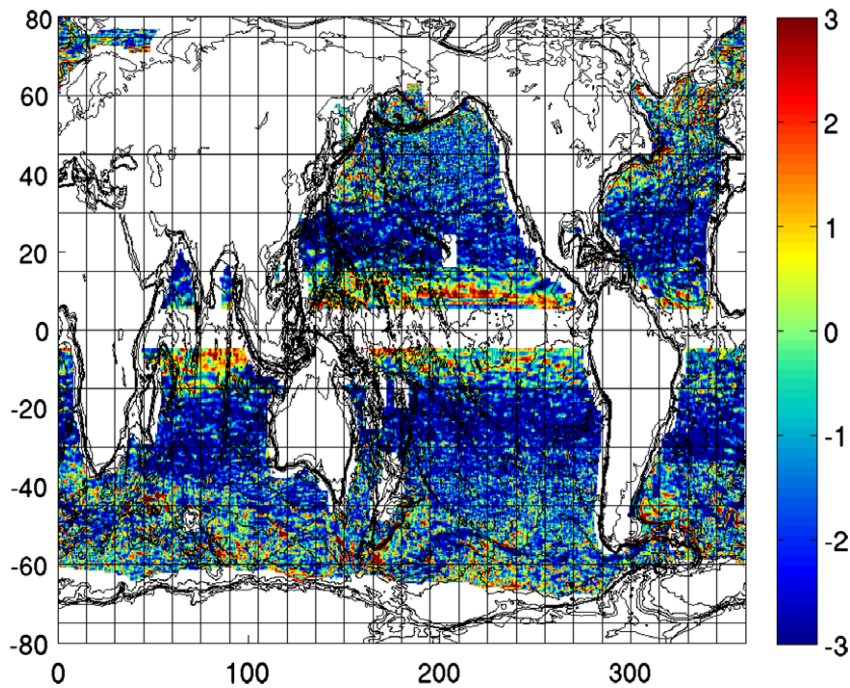


Fig. 3. Six-year mean $(u^2 - v^2)$ normalized by its standard error, for period January 2, 2000 through December 31, 2005, from satellite altimetry. A 105-day running mean was removed from u and v time series before calculating $(u^2 - v^2)$. Contours are bottom topography with CI = 1000 m. About 27% of the World Ocean is significant at the 2-sigma level, while 33% (15%) of the ocean poleward of 25° is significant at the 2-sigma (3-sigma) level.

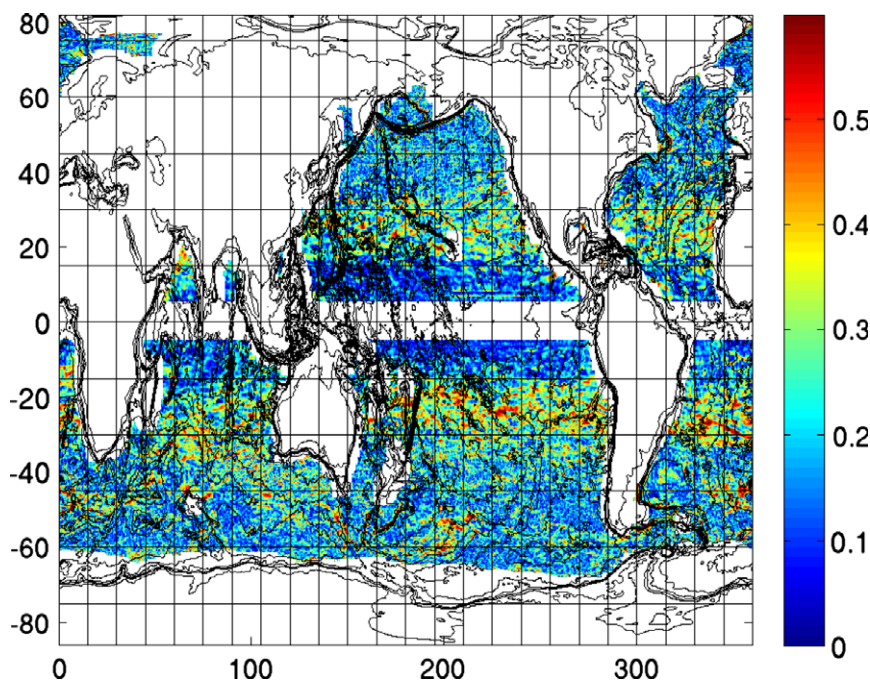


Fig. 4. Six-year mean M_n for period January 2, 2000 through December 31, 2005, from satellite altimetry. A 105-day running mean was removed, and spatial high-pass filter applied to u and v time series before calculating $(u^2 - v^2)$. Contours are bottom topography with CI = 1000 m. The spatial correlation of the field shown here with that found for the earlier 6-year period is $r = 0.33$ for depths greater than 1000 m.

extratropics. Their persistence is confirmed by the spatial correlation $r = 0.64$ between the fields in Figs. 6 and 7 for depth greater than 1000 m. Much of this persistence is due to the not surprising zonal bands in the Tropics. Removing this, we find the correlation poleward of 25° is $r = 0.50$. Given the enormous number of degrees of freedom, this is very highly statistically significant.

The mean M from Figs. 6 and 7 is also very significantly correlated with M from 13 years of altimetry shown in Fig. 1. For depths greater than 1000 m $r = 0.47$ and $r = 0.27$ for all latitudes and poleward of 25° , respectively. This is impressive agreement given the small-scale structure of M and the fact that the OfES model has some of the currents slightly shifted from their true positions.

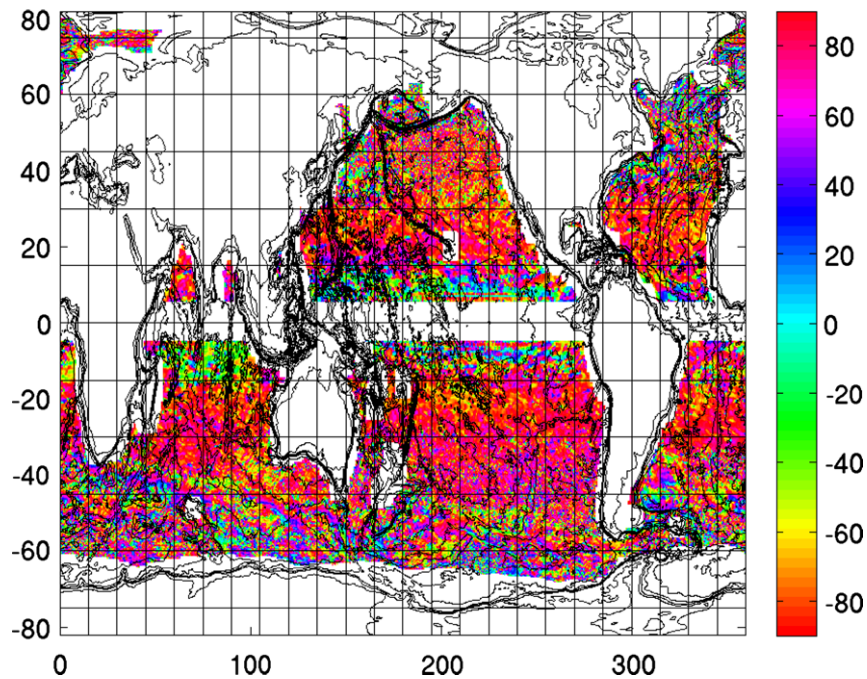


Fig. 5. Angle of the major axis of the covariance ellipse, measured anticlockwise from zonal, for data shown in Fig. 4. Contours are bottom topography with CI = 1000 m. The spatial correlation of the field shown here with that found for the earlier 6-year period is $r = 0.17$ for depths greater than 1000 m.

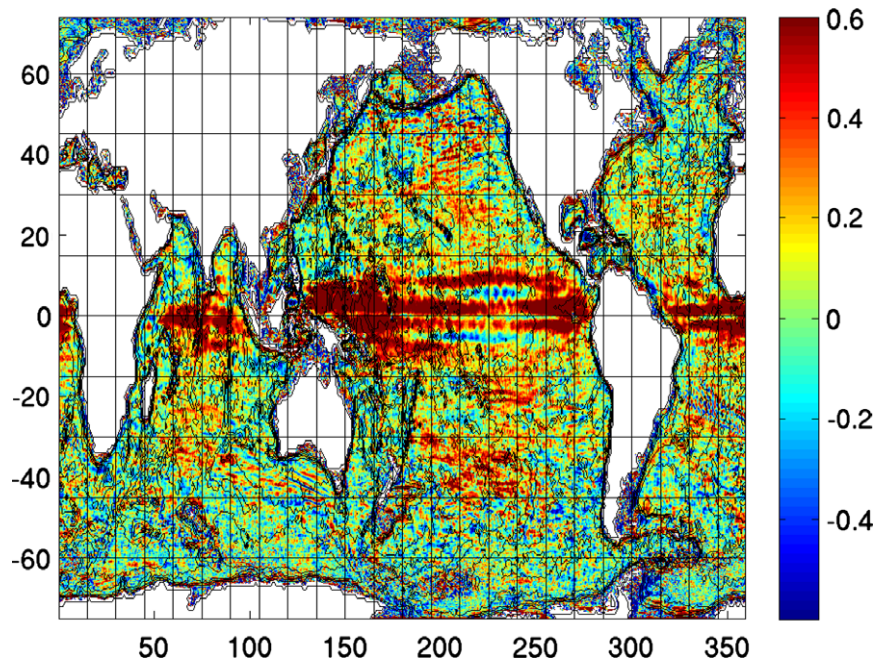


Fig. 6. Five-year average M from OfES model (simulation years 41–45). For depths greater than 1000 m, M is spatially correlated with M from the next five model years (see Fig. 7) at $r = 0.64$ globally and $r = 0.50$ for latitudes poleward of 25° . Higher correlations found when including all depths ($r = 0.75$ and 0.69 for the globe and extratropics, respectively). Contours are bottom topography with CI = 1000 m.

3.3. Idealized QG model

The persistence of the small-scale patchy structures in Figs. 1–7 is counter to one's intuition of the random, chaotic nature of turbulence that should eventually smear out any small-scale structures. To confirm this intuition, we calculated M from an idealized turbulence model (Arbic and Flierl, 2004b) meant to simulate a region of

the midlatitude ocean. We found small-scale patchy structures visually similar to that found in the real ocean, and confirmed that they are generated by coherent vortices. However, because the model is horizontally homogeneous, the model M fields (not shown here) *did not persist in time*. That is, M fields from two independent time periods, both 93 snapshots long, were statistically unrelated. (The correlation coefficient $r = -0.063$. Roughly, and

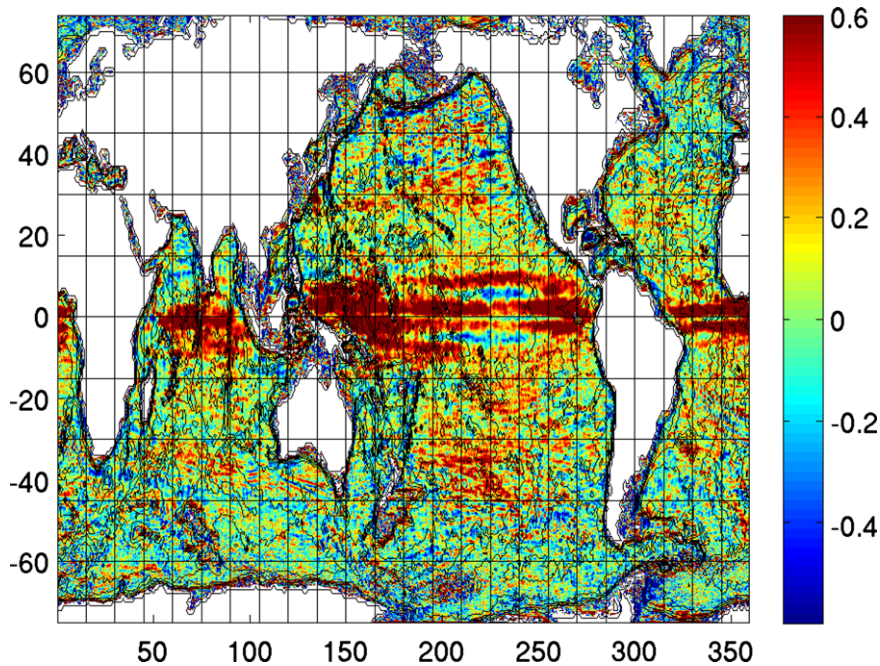


Fig. 7. Same as Fig. 6 but for simulation years 46–50.

generously, estimating the number of degrees of freedom at 625 from the plot of M , one expects this would occur from random fields with probability greater than 11%, and perhaps more often if the degrees of freedom are less than 625.) Of course this is to be expected from a homogenous turbulence model.

3.4. Length scales of anisotropic patches

In the Tropics it is clear that patches of positive M have greater zonal than meridional extent (Fig. 1). The situation is more subtle in the extratropics, and must be addressed quantitatively. We first found all the local maxima and minima in M poleward of 25° in Fig. 1 with $M > M_c$ (yellow to reddish patches) or $M < -M_c$ (bluish patches), respectively, where M_c is an arbitrary positive threshold. Then we found the zonal and meridional extent of the surrounding regions with $M > M_c$ or $M < -M_c$. For instance, the meridional extent was defined simply as the meridional distance from the most northerly point to the most southerly point. For the extratropical positive patches in Fig. 1 with $0.05 \leq M_c \leq 0.75$ we found mean zonal widths to be always larger than the meridional widths, see Fig. 8 red lines. (A qualitatively similar result holds for the two 6-year periods.) This is consistent with the fact that the longitudinal velocity autocorrelation drops off more slowly with separation distance than that for the transverse velocity in homogeneous, two-dimensional turbulence (Middleton and Garrett, 1986). For the blue patches, the relative sizes of the zonal and meridional widths depends upon M_c , see Fig. 8 blue lines. For large (small) M_c the mean meridional (zonal) scale is larger. Thus only the strong blue patches (large M_c) agree with simple turbulence theory. Something else must be invoked to understand the lighter blue patches (minima with small M_c). The greater zonal extent of the light blue patches is consistent with a predominant westward propagation of eddies. Because of the β -effect, vortices inherently propagate westward, with a slight equatorward (poleward) component for vortices rotating in the same (opposite) direction as Earth (McWilliams and Flierl, 1979; Morrow et al., 2004; Chelton et al., 2007), though the mean currents can redirect their paths (Fu, 2006).

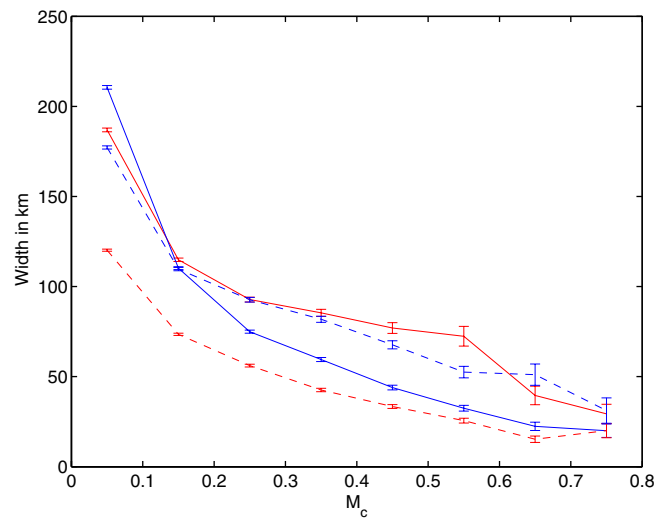


Fig. 8. Mean widths of extratropical patches of M , computed from satellite altimetry. Zonal widths (solid lines) and meridional widths (dashed lines) of patches with $M > M_c$ (red lines) and $M < -M_c$ (blue lines). Error bars represent the standard deviation over all patches divided by $\sqrt{N-1}$, where N is number of patches. Error bars increase with M_c due to fewer patches surpassing the larger thresholds.

3.5. Zonal averages of M

In Fig. 9a we plot the zonal average, $M_{z1} \equiv [M]$. A clear latitudinal dependence emerges that is consistent between the two time periods January 2, 1994 through December 31, 1999 (black line) and January 2, 2000 through December 31, 2005 (red line). The large positive values within the Tropics are consistent with the well known zonal currents and Rossby waves there. Note that the larger zonal than meridional decorrelation scale used for gridding the data in the Tropics (LeTraon et al., 1998) may tend to artificially suppress v variance, and increase M there. Despite this, M_{z1}

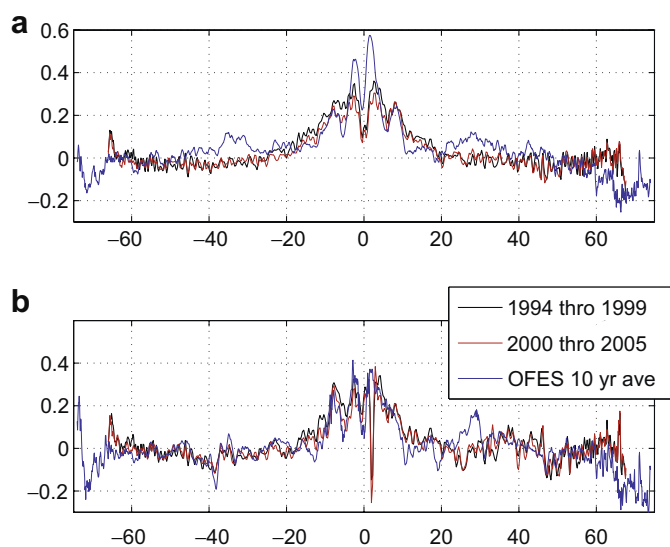


Fig. 9. (a) Zonal average of M , M_{z1} vs. latitude; (b) alternative zonal average, $M_{zz} = [(u^2 - v^2)/(u^2 + v^2)]$ vs. latitude. Region within a few degrees of the equator is suspect due to breakdown of geostrophic balance there.

from the last ten years of the OfES model, does not show a clear negative discrepancy in the Tropics (blue line).

In the midlatitudes in both hemispheres M_{z1} is small, and even slightly negative for both 6-year periods, see Fig. 9a. As mentioned previously, the altimeters capture the zonal currents better than the meridional currents for all but the high latitudes (at 56° the ascending and descending ground tracks are orthogonal for TOPEX/Poseidon and Jason; this occurs at higher latitudes for the other satellites (Chelton et al., 2001, Fig. 59)). Thus one might expect, if anything, the true M to be systematically even lower in the midlatitudes. Despite this, we find OfES had higher M there (blue line, Fig. 9a). Thus the OfES model is likely in error here. Furthermore, the slightly negative midlatitude M , consistent with the earlier results (Ducet et al., 2000), is in stark contrast to the theoretical ocean models that generally predict $u^2 \gg v^2$, so $M > 0$. (The dominance of zonal currents is visually apparent from individual snapshots, see for example Rhines (1975, Fig. 6), Panetta (1993, Fig. 7), Okuno and Masuda (2003, Fig. 1a).) This discrepancy clearly requires more attention.

As a starting point to explain the slightly negative midlatitude M we note that β is not necessarily dominant in the real ocean. Model simulations of fully developed QG turbulence (Arbic and Flierl, 2004a) with strong (weak) planetary β relative to that of the imposed mean shear-induced gradients of PV have large (small) positive M . However Arbic and Flierl (2004a) find M averaged over the model domain is always positive. So while weak β can account for small M , it cannot account for negative M .

Another factor potentially relevant to explain the slightly negative midlatitude M is that the flow may be closer to weakly nonlinear rather than fully developed turbulence. In a detailed analysis of the Subtropical Counter Current region of the South Pacific, Qiu et al. (in press) find that meridionally elongated eddies are generated by linear baroclinic instability in late winter and early spring (which would favor negative M). Qiu et al. (in press) also diagnosed the nonlinear interactions in this region. They found the subsequent nonlinear evolution over the summer and fall drives the eddy kinetic energy spectrum toward larger horizontal scale and preferentially zonally elongated modes. That is, there is an anisotropic inverse cascade driving the flow toward more zonal alignment (which favors more positive M). Interpreted from this mechanism, we speculate that the zonally averaged M results here

may reflect the degree to which the flow has had a chance to develop from linear instability into fully-developed turbulence. In particular, $[M] < 0$ suggests for most longitudes of the midlatitudes, the flow is more weakly nonlinear (or closer to linear instability) than fully developed nonlinear flow.

Similar results were obtained with the alternative zonal average $M_{zz} = [(u^2 - v^2)/(u^2 + v^2)]$, which gives more weight to regions of strong currents, see Fig. 9b, and is akin to the domain averages of Arbic and Flierl (2004a). The main difference between Figs. 9a and b is the larger fluctuations with latitude, for example negative extrema near 40°S, 25°N, and 45°N. Note also the positive maximum between about 30° and 40°N, a signature of the Gulf Stream and quite zonal Kuroshio Extension, both very energetic western boundary currents. Also the agreement with OfES is better.

4. Discussion of the origin of the patchy M field

The persistent, small-scale patches in Figs. 1–7 would arise if vortices consistently follow preferred paths in the ocean; see Fig. 10. But this raises the question as to the physical mechanism that could provide this memory in a flow that quickly forgets its initial conditions. The mesoscale eddies of the ocean are the dynamical equivalent of synoptic weather systems in the atmosphere, which are an order of magnitude larger. (The atmospheric mesoscale corresponds to a similar length scale, but it has much different dynamics.) Midlatitude synoptic weather systems are organized into well known storm tracks, due to nonlinear interaction between the mean flow and eddies of similar strength, and by large mountain ranges and land–sea temperature contrasts fixed in space. In the ocean the mean flow is much larger scale, and, in all but a few small regions, much weaker in strength, than the mesoscale eddy flow. Similarly the wind forcing is typically on scales much larger than the ocean mesoscale. (The time mean wind stress curl does show surprising small-scale structure near mountainous coastlines and the strong currents and temperature fronts of the major western boundary currents and Antarctic Circumpolar Current (Chelton et al., 2004).) But away from these areas are broad expanses of smoothly varying forcing field where, despite this, M has small-scale structure.) Thus neither the oceanic mean flow nor the atmospheric forcing can explain the persistent mesoscale patchy M .

Bottom topography of course remains essentially fixed in time from year to year, and does indeed influence ocean currents. For example, it has been observed that oceanic floats prefer to follow contours of f/H , where f is the Coriolis parameter and H is the total water depth, even for floats surprisingly close (around 100 m) to the surface (LaCasce, 2000). Indeed, studies that track the propagation of individual vortices have suggested that bottom topography west of the Perth Basin (near 105°E and 25°S) can steer anticyclones (Morrow et al., 2004). Thus it is tempting to speculate that the vortices might follow preferred paths due to steering by bottom topography. However, for a complete explanation, we would also need to know why eddies in a given region persistently end up on preferred f/H contours. At least in some parts of the highly equivalent barotropic Southern Ocean, the surface current variance ellipses appeared to be aligned with topography (Morrow et al., 1994). However, globally over the extratropical World Ocean, the angle of the major axis of the variance ellipse (see Fig. 5) is extremely weakly correlated, $r = 0.021$, with the direction of isobaths taken from Smith and Sandwell (1997). Furthermore, the degree of anisotropy measured by the eccentricity of the variance ellipse, M_n , (see Fig. 4) was extremely weakly correlated with the magnitude of the slope.

We performed a simulation with the idealized midlatitude ocean model used by Arbic and Flierl (2004b), with the only change

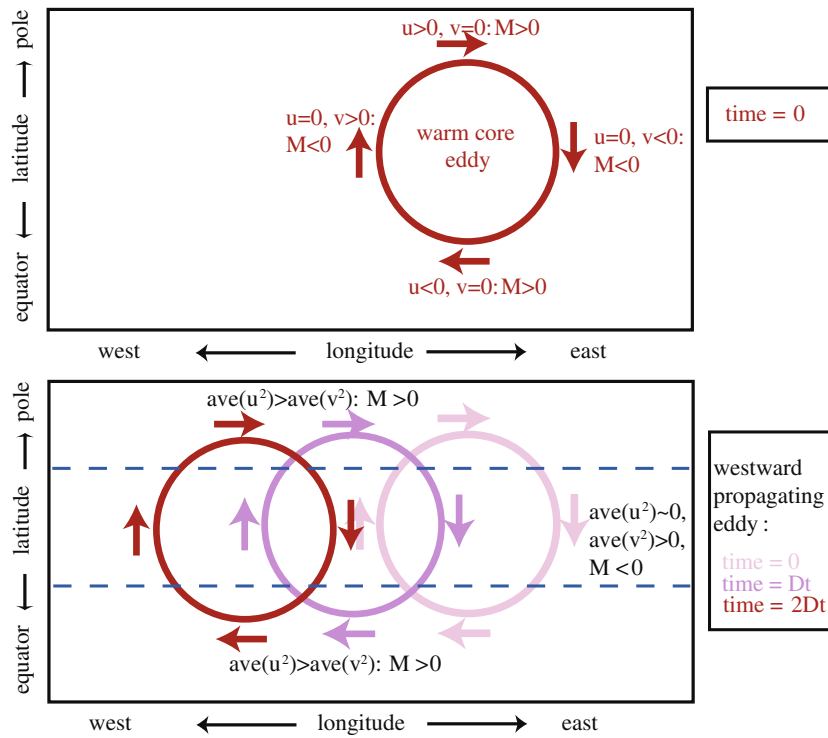


Fig. 10. If eddies tend to follow persistent paths, this would create the persistent streaks in the M field. In particular, $M > 0$ ($M < 0$) should appear on the flanks of routes of eddies moving more zonally (meridionally), and the centres of the routes should have $M < 0$ ($M > 0$). The mechanism is demonstrated here for an anticyclone in the Northern Hemisphere. But similar results apply in the Southern Hemisphere, and for cyclones.

being the inclusion of rough bottom topography, see contours in Fig. 11. The parameter settings were for their most realistic run $\delta = H_1/H_2 = 1/5$ and $TP = U/L_d R = 2.5$, where H_1 and H_2 are the equilibrium depths of the upper and lower layers, U is the imposed vertical shear between layers, L_d the internal deformation radius, and R the bottom friction parameter. The topography was taken from a bumpy region in the South Atlantic, made doubly periodic by reflections, and then scaled by 0.125. The scaling was found to be necessary for the model to equilibrate with reasonable spin up time. The M fields calculated from upper layer velocities for two independent time periods 150 snapshots long, were only weakly related, with spatial correlation between the two M fields of $r = 0.15$. The two M fields are shown in Fig. 11. While by eye they seem unrelated, if we guess that there are roughly 15^2 degrees of freedom, then a correlation of magnitude $r = 0.15$ occurs randomly only with probability 0.014. In other words, these seemingly weak correlations are in fact statistically significant at the 5% level. Regardless of the formal statistical significance, the QG model M fields are much less persistent than in the real ocean, where M fields averaged over different time periods were much more strongly correlated. Thus it appears unlikely that the organization of the turbulent vortices into persistent patchy M fields can be fully explained by simple steering of eddies along preferred paths by small-amplitude topography within quasigeostrophic dynamics. Possibly stronger topographic variations may lead to stronger persistence. Investigating the effects of the stronger topographic variations that violate QG but are typical of the real ocean will have to be explored with more general models.

5. Discussion

The implications of the upper ocean current anisotropy revealed by the 13-year, multi-satellite altimeter data are quite diverse. Previous studies have, as a working hypothesis, assumed the surface

eddy kinetic energy was isotropic (Stammer, 1997; Gille et al., 2000). The results found here show this assumption is gravely inappropriate locally. The most important implications for this will likely come from the adjustments that must be made to the parameterization of turbulent diffusion (important for the redistribution of tracers by the mesoscale flow, which is not resolved in state-of-the-art climate models). This will require extensive further study, but here we illustrate one simple result. For time periods shorter than the decorrelation time, the rate of spreading of a tracer from a single point (for instance, an oil spill) can be written as $\langle X(t)^2 \rangle = \langle u^2 \rangle t^2$, and $\langle Y(t)^2 \rangle = \langle v^2 \rangle t^2$, where $\langle X(t)^2 \rangle$ and $\langle Y(t)^2 \rangle$ are the mean squared displacements from the point of release in the zonal and meridional directions (Vallis, 2006). This implies, for example, that regions with $M = 1/2$ (deep red in Fig. 1) have mean squared zonal displacements three times those in the meridional direction. The description of turbulent fluxes of heat or tracers with spatially distributed sources is very complicated. We must integrate over times longer than the decorrelation time, and the tracer will visit many regions, which have very different M . Arguing heuristically we suspect the rate of spreading will depend upon area averaged anisotropy properties. Averaged over large regions isotropy seems to be almost applicable outside the Tropics. The slight but persistent negative zonally averaged M (between about -0.05 and -0.01) in midlatitudes may lead to more efficient meridional than zonal heat transport, but this requires further study to quantify. Climate models, which do not resolve the mesoscale processes, may need to parameterize this more efficient meridional transport. Finally, surface eddy kinetic energy, defined as $(u^2 + v^2)/2$, is an important, widely used diagnostic for the realism of high resolution ocean general circulation models. The anisotropy measure M provides a very different test of such models, in that M has much more small-scale structure than does the kinetic energy, and is not dominated by a few energetic regions such as western boundaries.

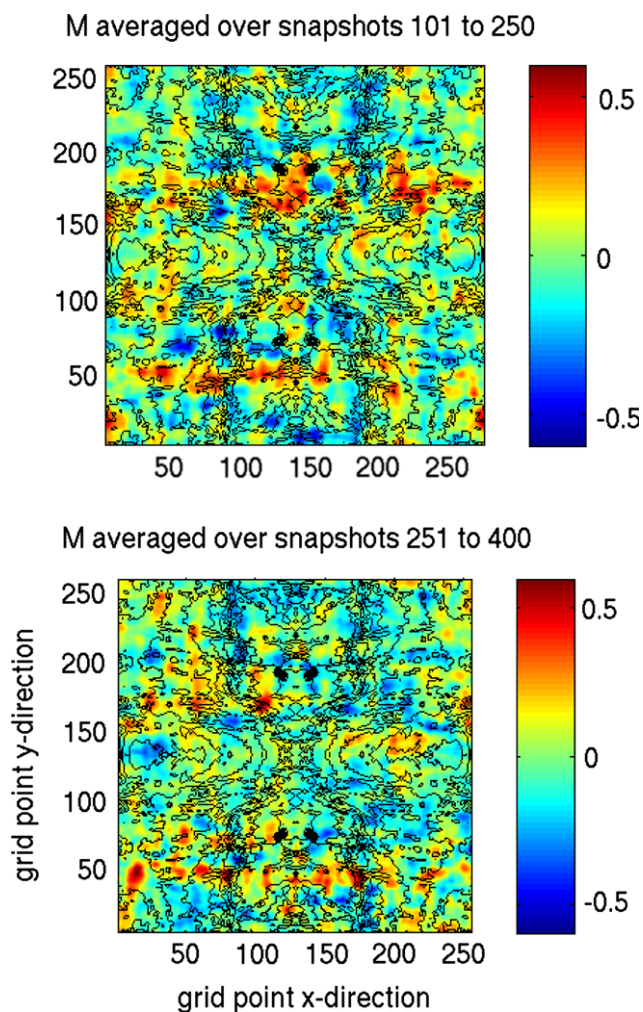


Fig. 11. Average M over 150 snapshots of the surface layer of a 2-layer, idealized QG model. The flat bottom model of Arbic and Flierl (2004b) was rerun with the bottom topography shown in black contours with $CI = 50$ m: (a) the 1st 150 snapshot period; (b) the 2nd 150 snapshot period. Spatial correlation between M in (a) and (b) is $r = 0.15$.

Acknowledgements

The altimeter products were produced by Ssalto/Duacs and distributed by Aviso, with support from Cnes. Bottom topography was a filtered version of Smith and Sandwell topography. OfES data provided by ESC/JAMSTEC. Dudley Chelton provided helpful comments on an earlier draft. We also benefitted from conversations with Greg Holloway, Bill Merryfield, and from two anonymous reviews. This paper is dedicated to the memory of the great physical oceanographer and journal editor Peter Killworth, who started its review process.

The authors acknowledge the Texas Advanced Computing Center (TACC) at The University of Texas at Austin for providing HPC resources that have contributed to the research results reported within this paper.

URL: <http://www.tacc.utexas.edu>. R.B.S. was supported by NSF Grant OCE-0526412. B.K.A. and C.L.H. were supported by a Jackson School of Geosciences Development Grant. BKA also received support from NSF Grant OCE-0623159. B.Q. was supported by NASA Contract 1207881. We thank the Jackson School of Geosciences for support. This is UTIG contribution #1981.

References

- Arbic, B.K., Flierl, G.R., 2004a. Effects of mean flow direction on energy, isotropy, and coherence of baroclinically unstable beta-plane geostrophic turbulence. *J. Phys. Oceanogr.* 34, 77–93.
- Arbic, B.K., Flierl, G.R., 2004b. Baroclinically unstable geostrophic turbulence in the limits of strong and weak bottom Ekman friction: application to midocean eddies. *J. Phys. Oceanogr.* 34, 2257–2273.
- Batchelor, G.K., 1953. *The theory of homogeneous turbulence*. Cambridge Monographs on Mechanics and Applied Mathematics. Cambridge University Press, Cambridge, UK. 197+xi pp.
- Chelton, D.B., Ries, J.C., Haines, B.J., Fu, L.-L., Callahan, P.S., 2001. Satellite altimetry. In: Fu, L.-L., Cazenave, A. (Eds.), *Satellite Altimetry and Earth Sciences: A Handbook of Techniques and Applications*. Academic Press, pp. 1–131.
- Chelton, D.B., Schlax, M.G., Freilich, M.H., Milliff, R.F., 2004. Satellite measurements reveal persistent small-scale features in ocean winds. *Science* 330, 978–983.
- Chelton, D.B., Schlax, M.G., Samelson, R.M., de Szoeke, R.A., 2007. Global observations of large oceanic eddies. *Geophys. Res. Lett.* 34. doi:10.1029/2007GL030812.
- Danilov, S.D., Gurarie, D., 2000. Quasi-two-dimensional turbulence. *Physics-Uspeski* 43, 863–900.
- Ducet, N., LeTraon, P.-Y., 2001. A comparison of surface eddy kinetic energy and Reynolds stresses in the Gulf Stream and the Kuroshio Current systems from merged TOPEX/Poseidon and ERS-1/2 altimetric data. *J. Geophys. Res.* 106 (C8), 16603–16622.
- Ducet, N., LeTraon, P.-Y., Reverdin, G., 2000. Global high-resolution mapping of ocean circulation from TOPEX/Poseidon and ERS-1 and -2. *J. Geophys. Res.* 105 (C8), 19477–19498.
- Fjortoft, R., 1953. On the changes in the spectral distribution of kinetic energy for two-dimensional non-divergent flow. *Tellus* 5, 225–230.
- Frisch, U., 1995. *Turbulence: The Legacy of A.N. Kolmogorov*. Cambridge University Press, New York. 296+xiii pp.
- Fu, L.-L., 2006. Pathways of eddies in the South Atlantic Ocean revealed from satellite altimeter observations. *Geophys. Res. Lett.* 33, L14610. doi:10.1029/2006GL026245.
- Galperin, B., Nakano, H., Huang, H.-P., Sukoriansky, S., 2004. The ubiquitous zonal jets in the atmospheres of giant planets and Earth's oceans. *Geophys. Res. Lett.* 31 (L13303). doi:10.1029/2004GL019691.
- Galperin, B., Sukoriansky, S., Dikovskaya, N., Read, P., Yamazaki, Y., Wordsworth, R., 2006. Anisotropic turbulence and zonal jets in rotating flows with a beta-effect. *Nonlinear Proc. Geophys.* 13, 83–98.
- Gille, S.T., Yale, M.M., Sandwell, D., 2000. Global correlation of mesoscale ocean variability with seafloor roughness from satellite altimetry. *Geophys. Res. Lett.* 27, 1251–1254.
- Hogg, N., 1988. Stochastic wave radiation by the Gulf Stream. *J. Phys. Oceanogr.* 18, 1687–1701.
- Huang, H.-P., Kaplan, A., Curchitser, E.N., Maximenko, N.A., 2007. The degree of anisotropy for mid-ocean currents from satellite observations and an eddy-permitting model simulation. *J. Geophys. Res.* 112 (C09005). doi:10.1029/2007JC004105.
- Jacobs, G., Barrow, C., Rhodes, R., 2001. Mesoscale characteristics. *J. Phys. Oceanogr.* 106 (C9), 19581–19595.
- Kistler, R.E., Kalnay, E.M., Collins, W., Saha, S., White, G., Woollen, J., Chelliah, M., Ebisuzaki, W., Canamitsu, M., Kousky, V., van den Dool, H., Jenne, R., Fiorino, M., 2001. The NCEP/NCAR 50-year reanalysis: monthly means CD-ROM and documentation. *Bull. Am. Meteorol. Soc.* 82, 247–267.
- LaCasce, J.H., 2000. Floats and f/h. *J. Mar. Res.* 58, 61–95.
- LeTraon, P.-Y., Dibarboure, G., Ducet, N., 2001. Use of a high-resolution model to analyze the mapping capabilities of the multi-altimeter missions. *J. Atmos. Ocean. Technol.* 18, 1277–1288.
- LeTraon, P.-Y., Nadal, F., Ducet, N., 1998. An improved mapping method of multisatellite altimeter data. *J. Atmos. Ocean. Technol.* 15, 522–534.
- Maximenko, N.A., Band, B., Sasaki, H., 2005. Observational evidence of alternating zonal jets in the World Ocean. *Geophys. Res. Lett.* 32 (12). Art. No. L12607.
- McDowell, S.E., 1986. On the origin of eddies discovered during the POLYMODE local dynamics experiment. *J. Phys. Oceanogr.* 16, 632–652.
- McWilliams, J.C., 1976. Maps from the mid-ocean dynamics experiment: Part I. Geostrophic streamfunction. *J. Phys. Oceanogr.* 6, 810–827.
- McWilliams, J.C., Flierl, G.R., 1979. On the evolution of isolated, nonlinear vortices. *J. Phys. Oceanogr.* 9, 1155–1182.
- Middleton, J., Garrett, C., 1986. A kinematic analysis of polarized eddy fields using drifter data. *J. Geophys. Res.* 91 (C4), 5094–5102.
- Morrow, R.A., Birol, F., Griffin, D., Sudre, J., 2004. Divergent pathways of cyclonic and anti-cyclonic ocean eddies. *Geophys. Res. Lett.* 31, L24311. doi:10.1029/2004GL020974.
- Morrow, R.A., Coleman, R., Church, J., Chelton, D., 1994. Surface eddy momentum flux and velocity variances in the Southern Ocean from GEOSAT altimetry. *J. Phys. Oceanogr.* 24, 2050–2071.
- Okuno, A., Masuda, A., 2003. Effect of horizontal divergence on the geostrophic turbulence on a beta-plane: suppression of the Rhines effect. *Phys. Fluids* 15, 56–65.
- Panetta, R.L., 1993. Zonal jets in wide baroclinically unstable regions – persistence and scale selection. *J. Atmos. Sci.* 50, 2073–2106.
- Pascual, A., Pujol, M.-I., Larnicol, G., LeTraon, P.-Y., Rio, M.H., Hernandez, F., 2007. Mesoscale mapping capabilities of multisatellite altimeter missions: first results with real data in the Mediterranean Sea. *J. Mar. Sys.* 65, 190–211.

- Puillat, I., Taupier-Letage, I., Millot, C., 2002. Algerian eddies lifetime can near 3 years. *J. Mar. Sys.* 31, 245–259.
- Qiu, B., Scott, R.B., Chen, S., in press. Length-scales of generation and nonlinear evolution of the seasonally-modulated South Pacific subtropic countercurrent. *J. Phys. Oceanogr.* 38.
- Rhines, P.B., 1975. Waves and turbulence on a β -plane. *J. Fluid Mech.* 69, 417–443.
- Rhines, P.B., 1977. The dynamics of unsteady currents. In: Goldberg, E. et al. (Eds.), *The Sea*, vol. VI. John Wiley & Sons, pp. 189–318. (Chapter 7).
- Sakuma, H., Sasaki, H., Takahashi, K., Tsuda, Y., Kanazawa, M., Kitawaki, S., Kagimoto, T., Sato, T., 2003. *NEC Res. Develop.* 44, 104.
- Schlax, M.G., Chelton, D.B., 2003. The accuracies of crossover and parallel-track estimates of geostrophic velocity from TOPEX/Poseidon and Jason altimeter data. *J. Atmos. Ocean. Technol.* 20, 1196–1211.
- Schmitz, W.J., 1988. Exploration of the eddy field in the midlatitude North Pacific. *J. Phys. Oceanogr.* 18, 459–468.
- Schmitz, W.J., Price, J., Richardson, P., 1988. Recent moored current-meter and sofar float observations in the eastern Atlantic near 32°N. *J. Mar. Res.* 46, 301–319.
- Smith, W.H.F., Sandwell, D.T., 1997. Global sea floor topography from satellite altimetry and ship depth soundings. *Science* 277, 1956–1962.
- Stammer, D., 1997. Global characteristics of ocean variability estimated from regional TOPEX/Poseidon altimeter measurements. *J. Phys. Oceanogr.* 27, 1743–1769.
- Vallis, G.K., 2006. *Atmospheric and Oceanic Fluid Dynamics: Fundamentals and Large-scale Circulation*. Cambridge University Press.
- Vallis, G.K., Maltrud, M., 1993. Generation of mean flows and jets on a beta plane and over topography. *J. Phys. Oceanogr.* 23, 1346–1362.
- Zang, X., Wunsch, C., 2001. Spectral description of low-frequency oceanic variability. *J. Phys. Oceanogr.* 31, 3073–3095.